Automated Assembly of Stacked Tracker Modules for the CMS Phase II Upgrade

Meadhbh Murphy, Trinity College Dublin

Supervisor: James Keaveney

18th July - 7th September 2017

Abstract

The planned upgrade of the LHC to the High Luminosity LHC will require an upgrade of the CMS tracker. To reduce the data volumes generated a stacked sensor module will be introduced which is capable of disregarding low transverse momentum particles. The development of an automated assembly procedure for stacked sensor modules is underway. This report outlines advances made in the important area of the relative angular alignment of the sensors in a stacked module. An automated procedure to detect two corners of a silicon sensor and use this to define its position and angular orientation has been developed. An iterative process to rotate the sensor to a predefined angular orientation has been introduced. Finally a dummy module was built with a relative angular alignment approaching that required for a PS (pixel-strip) module.

Contents

1 Introduction

1.1 The CMS Detector

The Compact Muon Solenoid (CMS) detector is a particle physics detector at the Large Hadron Collider (LHC) at CERN. It is built around a large solenoid magnet which generates a magnetic field of approximately 4T. The size of this solenoid restricts the size of the detector itself requiring that it is compact at a length of 21.5m and a diameter of 15m. The detector itself is made up of many layers as can be seen in Figure 1. Each layer of the detector is designed to detect different types of particle and their properties. The inner-most layer which is closest to the beam line and interaction point is the tracker. This consists of silicon pixel and strip detectors which precisely record the trajectory and momentum of charged particles. Tracks (trajectories) are reconstructed through a complex algorithm connecting the points at which a particle strikes the different layers of silicon sensors, while the momentum of a particle can be reconstructed by the bending of its trajectory in the magnetic field.

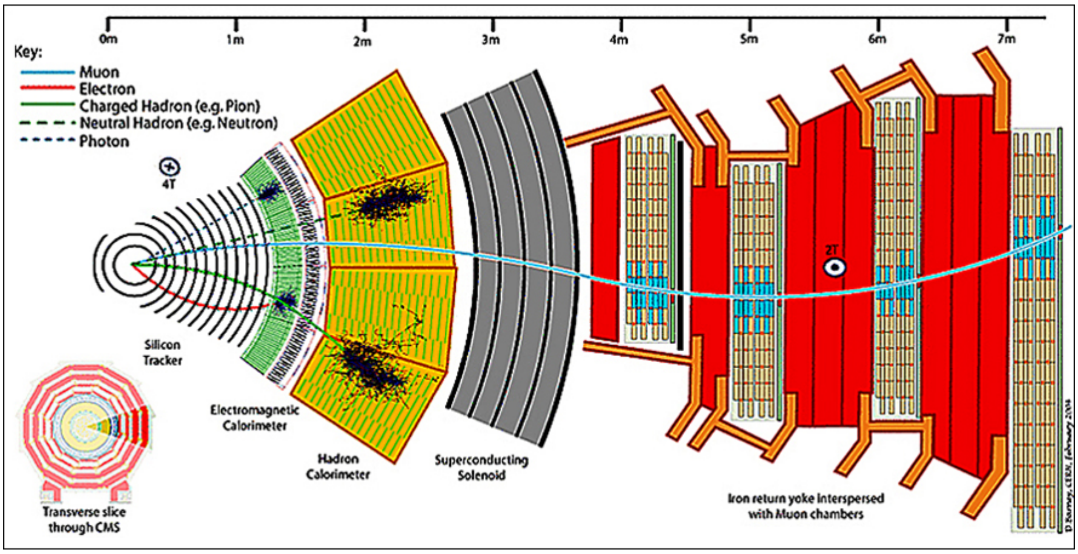

Figure 1: Cross Section of CMS Detector [1]

1.2 CMS Phase II Tracker Upgrade

The planned upgrade of the LHC to the High Luminosity LHC (HL-LHC) will require the upgrade of the current CMS tracker to deal with an increase in luminosity to approx $5 \times 10^{34} cm^{-2} s^{-1}$ and an integrated luminosity of $250 fb^{-1}$ per year for a further 10 years. [2] The move to HL-LHC will significantly increase the rate of bunch crossing to 40MHz, with each crossing resulting in approx 140 interactions.[2] This pose significant difficulties for not only the reconstruction of the particle trajectories but also the shipping of data off-detector at a rate of 40MHz. However many of the interactions that will be observed in HL-LHC are not of interest for new physics as they result in relatively light particles which are already well characterised.

1.3 Stacked Outer-Tracker Modules

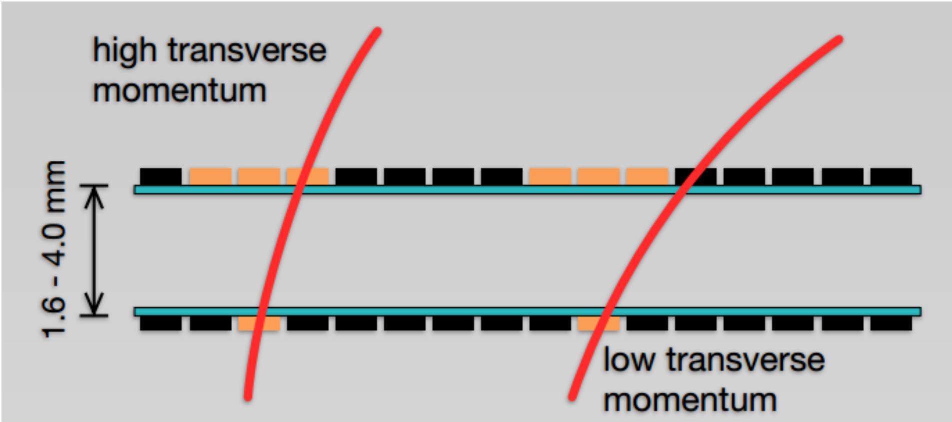

Figure 2: Stacked module with ability to disregard low p_T hits [3]

To reduce the amount of data generated and analysed the planned upgrade of the outer tracker will involve a "stacked module". These modules are capable of disregarding particles with low transverse momentum (p_T), which are not of interest for new physics. The concept revolves around the use of two closely spaced silicon sensors with common electronics in one module as shown in Figure 3. Two types of stacked module are planned. The first is a pixel-strip module (PS module) consisting of a silicon strip sensor and a silicon pixel sensor. The second type is a two strip module (2S module) which consists of two silicon strip sensors. This project concentrates on the automated assembly of the PS module, however both types of modules operate under the same principle. The curvature of a particle's trajectory can be determined, by comparing the position at which it strikes the inner sensor and then the outer sensor as illustrated in Figure 2. Given that the trajectory of a charged particle in a magnetic field is related to the mass of the particle, the curvature of the trajectory can be used to determine the particle's transverse momentum. The lower the transverse momentum a particle has the more curved its trajectory will be. It is then possible to define an "acceptance window" or region in the outer sensor as shown in Fig 2. If the particle strikes the outer sensor outside of this acceptance window it can be disregarded as a low p_T particle. By altering the distance between the sensors and the size of the acceptance window it is possible to tune the threshold below which particles are considered as low p_T. The threshold is planned to be set at approximately 2GeV which would correspond to a reduction of data volumes by an order of magnitude [2].

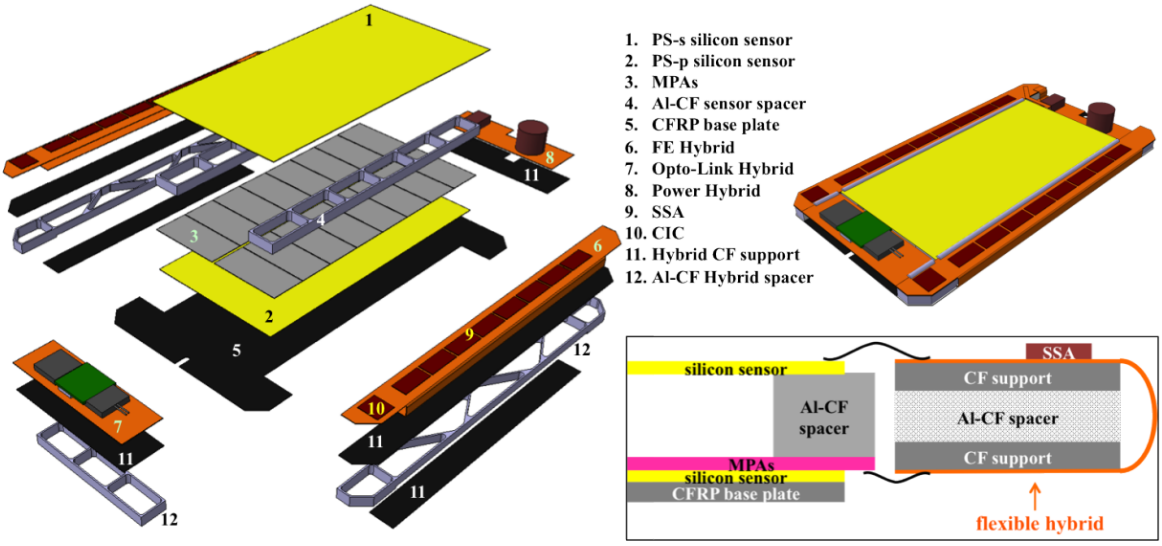

Figure 3: Structure of a pixel-strip (PS) module [2]

1.4 Automated Assembly

Given the large number of modules required for the phase 2 tracker upgrade it is clear that an automated assembly method would reduce time and labour required to manufacture these modules. Another advantage of the automated assembly of the module is an extreme control of the precision to which two sensors are aligned. For effective differentiation of low p_T and high p_T particles using a PS module it is demanded that the two sensors align to within $40\mu m$ as measured at the sensor's short edge. This corresponds to a relative rotational alignment to within $800\mu rad$ ($\approx 0.04°$). This is hoped to be achieved through a precise angular alignment step in assembly process.

2 Assembly Equipment and Software

2.1 Hardware

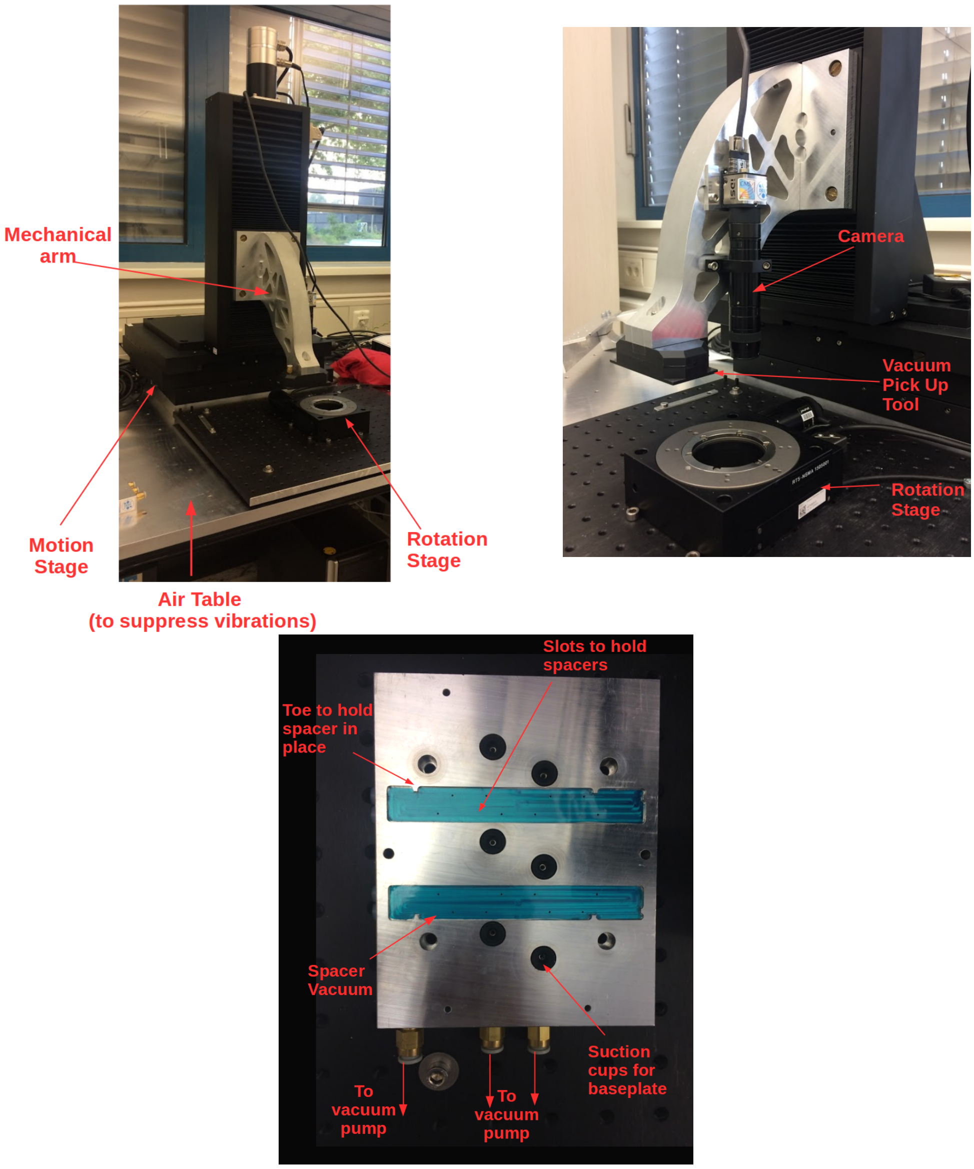

Figure 4: Equipment used in assembly procedure

The equipment in place for the assembly of stacked PS modules consists of:

- a motion stage with motion in x, y, z directions to a precision of 0.005mm
- a rotation stage with precision of 0.01 degrees

- a custom build robot arm
- a mobile camera mounted on the robot arm
- a vacuum pick up tool also mounted on the robot arm
- a custom built assembly platform with slots for the positioning of spacers, and vacuum suction cups to secure the position of spacers and the baseplate during assembly

2.2 Software

The motion stage, camera and vacuum system are all controlled by a user interface developed using a Qt framework with C++.

2.2.1 Pattern Recognition

A pattern recognition algorithm which identifies a corner of the silicon sensor was used throughout this project. The corners of a silicon sensor are identifiable by fiducial markers as shown in Figure 5

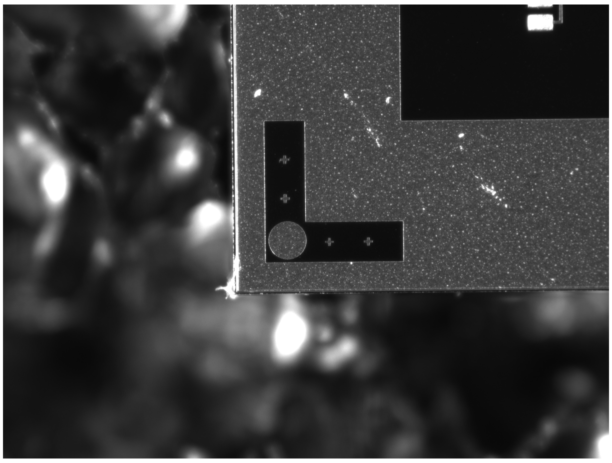

Figure 5: Ficidual marker found at the corner of silicon sensor

A raw image (the master image) is captured by the camera. This image is thresholded to mitigate the effect of random noise such as dust or ambient lighting conditions.This is a process in which all pixels with intensity less than the threshold value are set to black while those above the threshold are set to white. A template matching algorithm is then used to compare this image to a template image of the fiducial marker. The normalised square difference of pixel intensities of coincident pixels in the master and template image are used as a figure of merit. These values are calculated as the template image is moved through the master image and the minimum of this figure of merit corresponds to the best fit between the master and template images. Once the marker has been identified this process is repeated with the rotation of the template image to determine the angular orientation of the marker in the image as demonstrated in Figures 6 and 7.

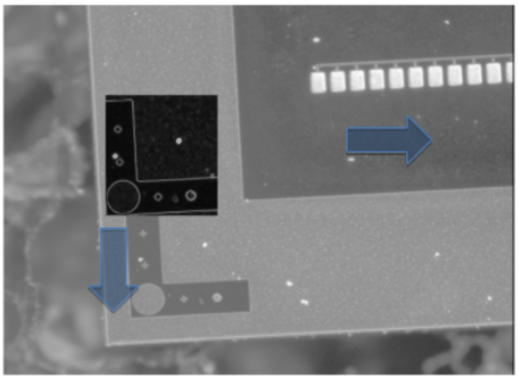

Figure 6: Pattern recognition

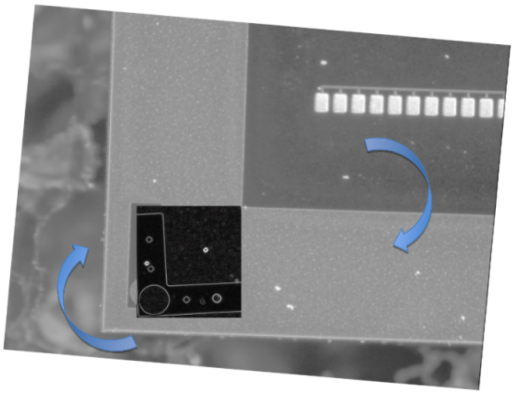

Figure 7: Pattern recognition

3 Proposed Assembly Process

The following steps are envisaged as part of the assembly procedure of the baseplate-sensor-spacer-sensor sub module:

1. Two aluminium spacers are manually placed in the spacer slots of the assembly platform and secured in place by the vacuum.
2. The top sensor is picked up using the vacuum pick up tool before being lowered and glued onto the spacers.
3. The angular orientation of the top sensor is detected.
4. The top sensor and spacers are picked up by the vacuum pick up tool and held above the assembly platform.
5. A baseplate is mounted on the platform.
6. The bottom sensor is glued in position onto the baseplate.
7. The orientation of the bottom sensor is detected.
8. The bottom sensor is brought to the same angular orientation as the top sensor using the rotation stage.
9. The top sensor is moved in the xy plane so that the centre of the two centres coincide.
10. The top sensor is lowered and glued to the bottom sensor.

This project concentrated on implementing the detection of the orientation of a sensor and the application of an angular correction to bring a sensor to a predefined angular orientation.

4 Finding Opposite Corners of a Sensor

An algorithm was developed to automatically locate the opposite corner of the sensor. The camera is manually brought to one corner marker and an image is taken. Pattern recognition is used to obtain the precise position (x_1, y_1) of the marker and its orientation in the xy plane. The angular orientation of the marker combined with the dimensions of the sensor are then used to calculate the translations Δx and Δy needed to bring the camera to the opposite corner. An additional correction is needed to ensure the entire opposite fiducial marker is contained in the camera's frame of view due to the rotation of the fiducial marker through 180° at opposite corners. The position of this second corner (x_2, y_2) is then found using pattern recognition.

5 Orientation of a Sensor

5.1 Defining the orientation of a sensor

In order to achieve precise relative alignment between the two sensors in a module it is necessary to accurately determine a sensor's position and angular orientation in the xy plane. The orientation and position of the sensor are defined using the position of two opposite corners and the slope of the line connecting them as illustrated in Figure 8. The midpoint of the diagonal line

$$(x_c, y_c) = (\frac{x_2 + x_1}{2}, \frac{y_2 + y_1}{2}) \tag{1}$$

was chosen to define the position of the sensor. The orientation of the sensor is extracted from the slope of the diagonal.

$$m = \frac{y_2 - y_1}{x_2 - x_1} \tag{2}$$

Once the position of the two opposite corners are well know the slope and midpoint of the line connecting them can be easily calculated.

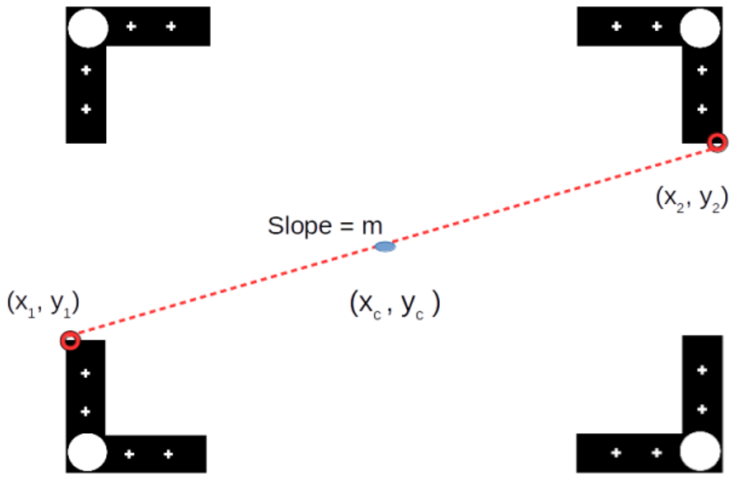

Figure 8: Orientation of silicon sensor with fiducial markers

5.2 Bringing the sensor to a predefined orientation

Once the orientation of a sensor is know the angular correction $\Delta\theta$ needed to bring it to a predefined angular orientation is calculated by taking the inverse tangent of slope of the sensor and taking the difference between.

$$\Delta\theta = \arctan\left(m_{target}\right) - \arctan\left(m\right) \tag{3}$$

In the context of the assembly procedure, the bottom sensor of the module will be brought to the previously detected orientation of the top sensor (m_{target}). However it was observed that when large angular corrections are applied through the rotation stage the sensor's corner marker often moved partially or completely out of the camera's frame of view. The rotation stage's axis of rotation is at the centre of the sensor as illustrated in Figure 9 so the rotation of the sensor results in a translation of the corner. This posed a considerable problem as if the corner marker is not completely contained in the image passed to the pattern recognition algorithm, it can not be correctly identified by the software.

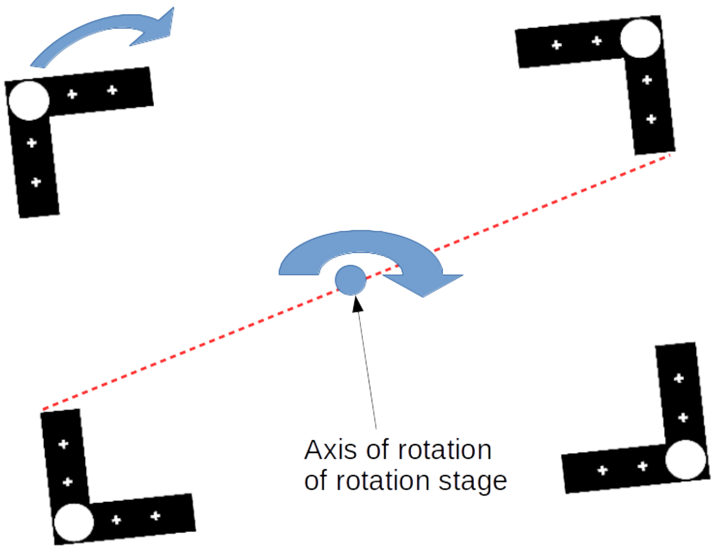

Figure 9: Axis of rotation of rotation stage

To resolve this issue the first solution considered was to calculate the the translation of the fiducial marker generated by the rotation of the sensor and then move the camera to the corner marker's new rotated position. However it was quickly realised that this would require the position of the centre of the sensor relative to the centre of the rotation stage was precisely known. Unfortunately this could not be easily implemented. To avoid this the iterative process described in Figure 10 was developed. The orientation of the sensor is determined and the angular correction $\Delta\theta$ required to bring the sensor to a predefined orientation is calculated. If this angular correction is larger than the maximum rotation $\Delta\theta_{max}$ which ensures the entire marker remains in the camera's view, the sensor is rotated by $\Delta\theta_{max}$. If the correction $\Delta\theta$ is less than $\Delta\theta_{max}$ the entire correction is applied in one step. The camera is then moved so that the fiducial marker lies in the centre of its field of view. This procedure is then repeated until the angular correction $\Delta\theta$ is less that the resolution of the rotation stage, which is 0.01°.

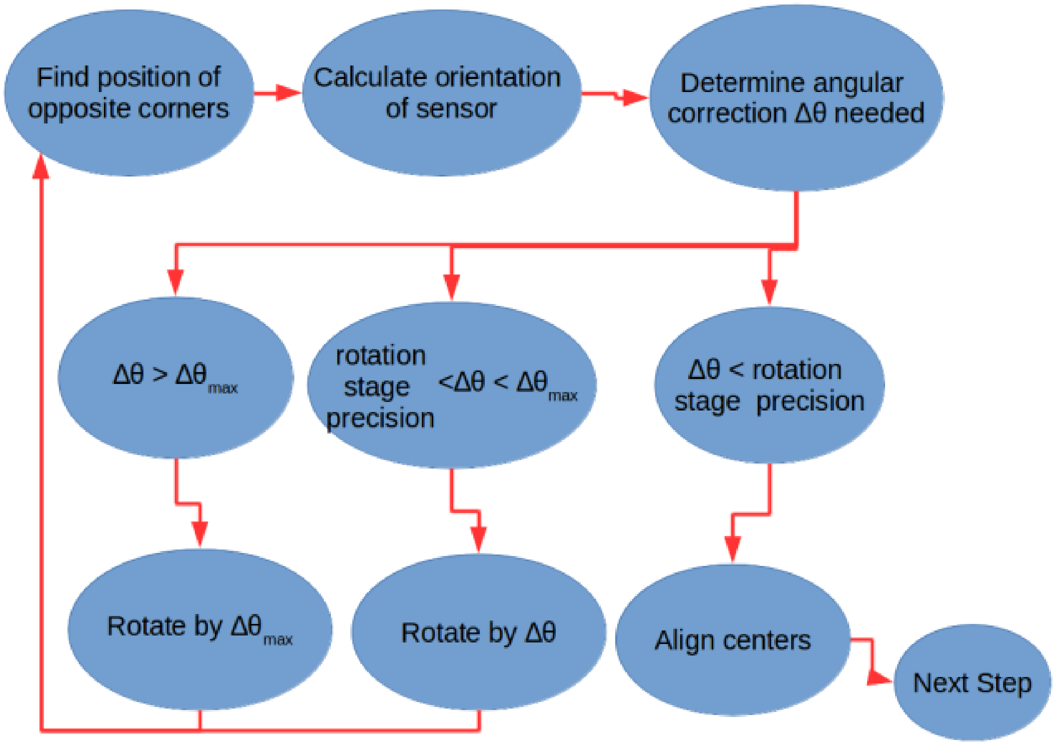

Figure 10: Flow diagram

6 Building a prototype

As sensors made of silicon are costly, an alternative dummy sensor was needed to build a prototype module and test the accuracy of the auto-alignment step.

6.1 Glass dummy

The first dummy sensor alternative tested were glass plates with painted silver corners as shown in Figure 11. The dimensions of the dummy were measured and were inputted into the code. However the glass dummies posed a few problems. Firstly the transparency of the glass increased the amount of noise obtained in images of the corners. Unlike with a silicon dummy sensor, light which was reflected off of the silver aluminium assembly platform passed through the glass dummy and increased the noise observed in images of the corners. Also the corner markers on the glass were "simple" corners as can be seen in Figure 12. They did not have any distinctive markings for the pattern recognition to identify. While pattern recognition proved capable of identifying the corner of the dummy, the rotational alignment obtained was not stable enough for the iterative alignment procedure to converge on a target angular alignment.

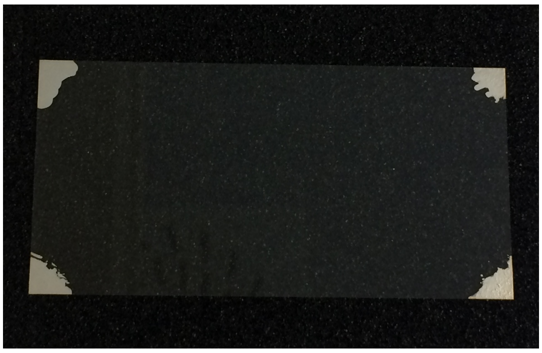

Figure 11: Glass dummy with silver painted corners

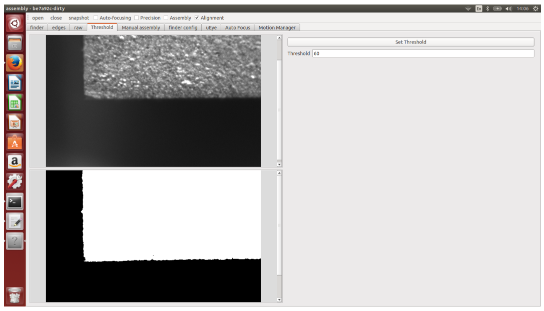

Figure 12: Simple corner

6.2 Silicon piece on glass dummy

6.2.1 Construction

To overcome the issues with the glass dummy sensors scrap pieces of silicon sensor were cut down to size and mounted on glass plates as illustrated in Figure 13. The scrap pieces of silicon used have fiducial markers and but were not of an appropriate size to be used in the assembly procedure, thus requiring them to be glued to dummy glass plates.

To allow the pick up tool to properly attach to the top sensor without any obstructions it was necessary to glue the piece of silicon to the underside of the glass. Therefore any images taken of these silicon marker were taken through the glass plate and a layer of glue. Transparent glue was used. However some impurities, which appear to be air bubbles, partially obscured the fiducial markers as seen in Figure 14. This initially lead to some instability in the results of the pattern recognition. Fortunately the fiducial markers on the silicon pieces contained additional marker components such as a pale capital F in a small dark square next to the original L shaped marker. By adding this to the template image and making some small adjustments to the focusing and thresholding of the image, the effects of the obscuring air bubbles were mitigated, and the iterative auto alignment procedure succeeded in bring the sensor to a predefined orientation.

Figure 13: Silicon piece mounted on glass plate

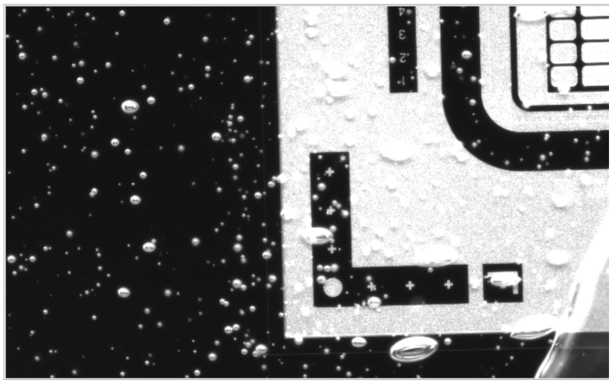

Figure 14: Air bubbles in glue obscuring fiducial marker

A dummy module was constructed bringing the two pieces of silicon to the same angular orientation. The top sensor-plate was placed on spacers in the assembly platform. It was brought to a predefined orientation. The sensor was then picked up by the vacuum tool and glue was placed on the spacers. The Top sensor plate was then lowered down onto the spacers and the glue was allowed to cure for approximately 15 mins with the vacuum pick up tool holding the sensor plate in place. The vacuum tool was then used to pick up the top sensor-plate and spacers. The bottom sensor was then placed upon two additional spacers in the assembly platform which acted as a platform above the baseplate vacuum suction cups. The orientation of the bottom sensor was detected and it was iteratively brought to the same orientation of the upper sensor plate. As the silicon was mounted on the glass in an uncontrolled manner, translational alignment of the glass plates was carried out by observation, ensuring that the silicon pieces did not shadow each other. Glue was then applied to the underside of the spacers attached to the top sensor plate, before it was lowered onto the bottom sensor. The glue was allowed to cure for 15 mins before the vacuum pick up tool was used to move the module dummy off of the assembly platform.

6.2.2 Metrology

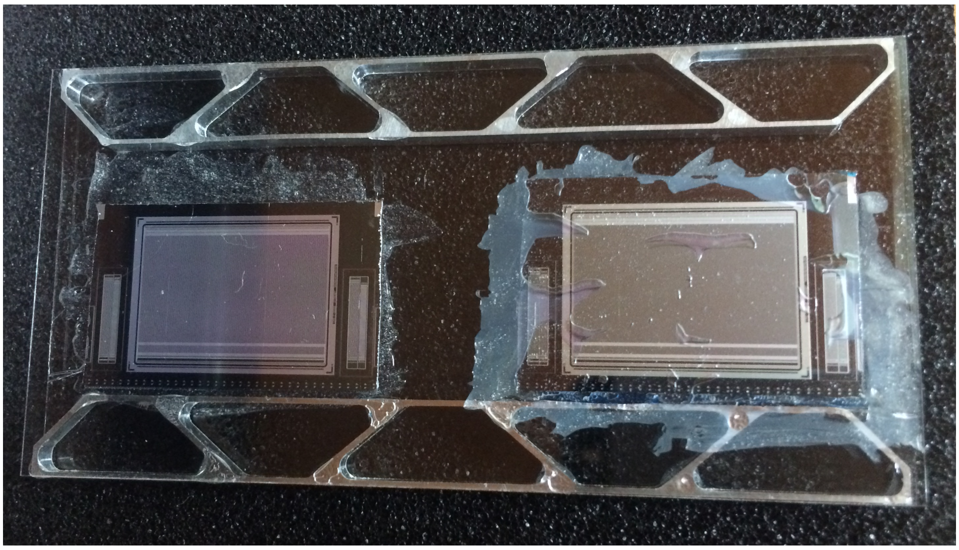

Figure 15: Dummy module

The dummy module constructed can be seen in Figure 15. To check the relative angular alignment of the two silicon pieces the orientation detecting algorithm was used to detect the orientation of the two pieces independently and then the relative misalignment between the silicon pieces was calculated. This was repeated 30 times and the results were plotted in a histogram as can be seen in Figure 16.

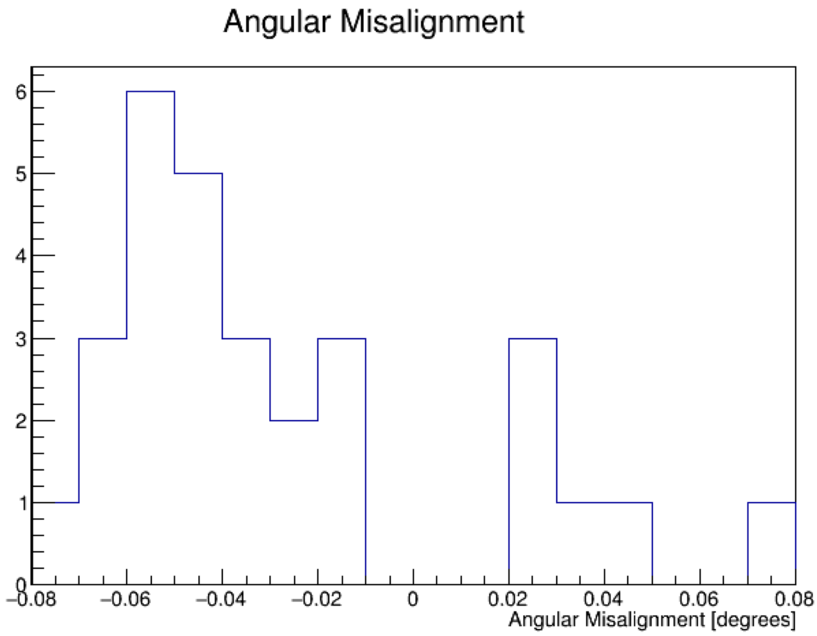

Figure 16: Relative misalignment of silicon pieces

A clear peak can be observed at a misalignment of $-0.05°$ which is approaching the precision required. However the accuracy of the orientation determining algorithm, which is limited by the size of the sensor being used and the resolution of the xy motion stage. The motion stage has a precision of $5\mu m$ in both x and y position. The error this introduces into the angular orientation detection is $0.02°$ for the small silicon pieces. This offers a an explanation of spread of results obtained, however this inaccuracy would be significantly reduced as the size of the silicon piece increases. For a PS module sensor sizes will be approx $50 \times 100mm^2$ [2] the error in the orientation detection would be reduced to approx $0.006°$. The measurements which can be seen further from the peak of the histogram can be explained by the sensitivity of the pattern recognition software to the ambient lighting conditions and the quality of the images used. The air bubbles in the glue would exaggerate effects due to changes in ambient lighting .

7 Conclusion

A number of developments in the automated assembly procedure of stacked sensor module for the CMS Tracker Phase 2 Upgrade have been made over the course of the summer student programme. An automated procedure has been put in place which locates two opposite corners of a sensor and uses these two points to define the position and angular orientation of the sensor. An iterative process to bring a sensor to a predefined angular orientation has been developed. A dummy module has been constructed using pieces of silicon sensors mounted on glass plates. The relative angular alignment of these silicon pieces was found to be approaching the precision required for a PS module and areas for the improvement of this relative misalignment have been identified.

8 Acknowledgements

I would like to sincerely thank my supervisor James Keaveney for all his help and direction during my time working on this project. I would also like to express my gratitude to Carsten Muhl for cutting the silicon pieces for the dummy module down to size. Finally I would like to especially thank the summer student program organisers for all their hard work ensuring our time here was enjoyable and instructive.

References

[1] Interactive Slice of the CMS detector, CMS-OUTREACH-2016-027 *S. Davis (CERN), CMS Collaboration*

[2] Technical Proposal for the Phase 2 Upgrade of the Compact Muon Solenoid *CMS Collaboration*

[3] Test beam results of the first CMS double-sided strip module prototypes using the CBC2 read-out chip *A. Harb, A. Mussgiller, J. Hauk et al (CMS Collaboration)*